Journal of Solid State Chemistry **153,** 132–139 (2000)
doi:10.1006/jssc.2000.8762, available online at http://www.idealibrary.com on IDEAL®

Structural Study of Electrochemically Obtained $Li_{2+x}Ti_3O_7$

M. E. Arroyo y de Dompablo,* A. Várez,† and F. García-Alvarado‡,[1]

*Departamento de Química Inorgánica, Facultad de CC. Químicas, Universidad Complutense de Madrid, 28040 Madrid, Spain;
†Departamento de Materiales, Escuela Politécnica Superior, Universidad Carlos III de Madrid, C/ Butarque 151, 28911 Leganés, Spain; and
‡Departamento de Química Inorgánica y Materiales, Facultad de Ciencias Experimentales y Técnicas, Universidad San Pablo-CEU, Urbanización Montepríncipe, 28668 Boadilla del Monte, Spain

Received March 6, 2000; in revised form April 27, 2000; accepted May 4, 2000; published online July 7, 2000

$Li_2Ti_3O_7$, a ramsdellite-type compound, is able to reversibly insert approximately 2.3 lithium ions per formula down to 1 V versus lithium. Both electron and X-ray diffraction techniques show that the electrochemically inserted compounds $Li_{2+x}Ti_3O_7$, with $x<2$, maintain the ramsdellite structure, although some important microstructural differences are observed. For example the compound with $x=0.55$ exhibits an incommensurate modulation ($q \approx \frac{1}{3}c^*$). On the other hand, for $Li_{2+x}Ti_3O_7$ with $x>2$, a commensurable $a \times 2b \times c$ cell can be proposed. A close structural relationship between the intercalated compounds and host compound, together with the small changes in the basic ramsdellite cell parameters during the intercalation process, is likely at the origin of the good cycling behavior of a lithium cell using $Li_2Ti_3O_7$ as the positive electrode. © 2000 Academic Press

Key Words: **lithium intercalation; electrochemical measurements; electron diffraction; structural characterization.**

INTRODUCTION

The compound $Li_2Ti_3O_7$ ($Li_{2.29}Ti_{3.43}O_8$ when referred to its unit cell) presents a ramsdellite-type structure (1,2) built up by double edge-sharing octahedral chains along the [001] direction. The chains are interconnected through corners in the *ab* plane (Fig. 1). This skeleton forms rectangular, 1×2 octahedra, tunnels running parallel to the *c* axis where some crystallographic sites are partially occupied by lithium ions, leading to the following composition per unit cell:

$$(Li_{1.72}\square_{2.28})^{\text{tunnel}}\,[(Li_{0.57}Ti_{3.43})O_8]^{\text{framework}}$$

The open framework of $Li_2Ti_3O_7$ allows for the insertion of lithium ions by both chemical and electrochemical means (3–5). In a previous paper (5), we proved that the composition $Li_{4.24}Ti_3O_7$ is reached by electrochemical lithium insertion down to 1 V versus lithium under near-equilibrium conditions. Once lithium ions have been inserted, they can be completely removed from the compounds $Li_{2+x}Ti_3O_7$ ($0 < x \leq 2.24$), leading back to the parent oxide $Li_2Ti_3O_7$ (3,5). Since $Li_{4.24}Ti_3O_7$, i.e., the highly lithiated compound $((Li_{4.28})^{\text{tunnel}}[(Li_{0.57}Ti_{3.43})O_8]^{\text{framework}}$ in terms of the ramsdellite unit cell), exceeds the composition limit of the ramsdellite structure, $A_4M_4O_8$ (6), the structural relationship between the host ($Li_2Ti_3O_7$), the intermediates ($Li_{2+x}Ti_3O_7$), and the final compound ($Li_{4.24}Ti_3O_7$) should clarify some aspects about the intercalation chemistry of this ramsdellite-type compound and its usefulness as an electrode of lithium cells.

As previously reported (5), the excellent reversibility of the intercalation reaction of lithium in $Li_2Ti_3O_7$ makes this compound attractive as an electrode material in rechargeable lithium batteries. In this sense, the compound could develop a maximum theoretical specific capacity of 235 A h/kg, which is an acceptable value for an electrode material. Besides, the relatively low average voltage of the intercalation reaction, 1.4 V versus Li^+/Li, points to $Li_2Ti_3O_7$ as a negative electrode for rocking chair batteries. In such a case the loss of specific energy due to the use of this ramsdellite instead of either carbon or coke as the negative electrode may be alleviated if the recently developed 5 V cathode materials (7) are used as the positive electrode. The viability of this application requires both a better knowledge of the insertion reaction and an understanding of the cycling behavior. We aim to show that ramsdellite suffers a low internal strain upon intercalation that may be the origin of the good cycling behavior. With this aim in mind, in this work we have characterized the phases formed during the intercalation reaction. The cell changes through the insertion reaction as well as the relationship between the parent and the highest lithiated compounds have been also investigated.

EXPERIMENTAL PROCEDURES

The starting $Li_2Ti_3O_7$ powder was synthesized as previously reported (3). Electrochemical experiments were

[1]To whom correspondence should be addressed. Tel: + 34 913724728. Fax: + 34 913510475. E-mail: flgaal@ceu.es.

0022-4596/00 $35.00

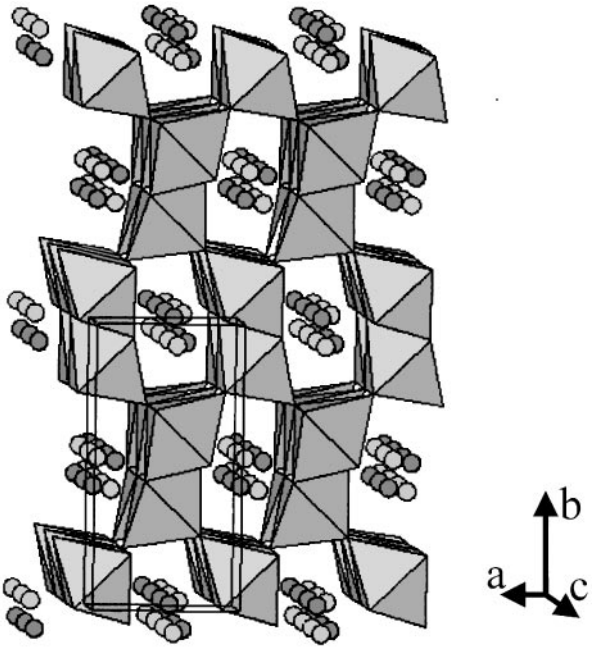

FIG. 1. Schematic representation of the ramsdellite-$Li_2Ti_3O_7$ framework. Circles in the tunnels denote the interstitial positions partially occupied by lithium ions.

performed using Swagelok cells bearing metallic lithium as the negative electrode. For the positive electrode, 5-mm diameter pellets made from a mixture of $Li_2Ti_3O_7$, carbon black, and ethylene-propylene-diene-terpolymer (EPDTP) were used. The electrolyte used was a 1 M solution of $LiClO_4$ in ethylene carbonate (EC) and diethoxyethane (DEE) (50:50 by volume). Cells were assembled in an argon-filled glove box and then connected to a multichannel MacPile system (8).

In order to determine the compositional range of the different $Li_{2+x}Ti_3O_7$ phases, a Step Electrochemical Potential Spectrum was collected from a cell with configuration Li/1 M $LiClO_4$ in DEE + EC (50:50 by volume)/$Li_2Ti_3O_7$ + C + EDPTP (89%, 10%, 1% w/o, respectively) at a discharging rate of 5 mV/h down to 1 V. Later on, several phases with compositions $Li_{2+x}Ti_3O_7$ were isolated by electrochemical lithium insertion in pellets conformed from a mixture of $Li_2Ti_3O_7$ and EPDTP in a 99:1 weight ratio. Different cells bearing $Li_2Ti_3O_7$ as the active material of the positive electrode were discharged up to the desired compositions of $Li_{2+x}Ti_3O_7$, with x ranging from 0.1 to 2.2. These experiments were performed under galvanostatic intermittent titration conditions using a current intensity of 0.1 mA/cm^2 during 0.2 h, and afterward allowing the cells a relaxation of 4 h before the next current pulse was applied. Cells were disassembled inside a glove box filled with argon, and the pellets were ground and dispersed in dry *n*-hexane for microstructural characterization. Electron diffraction patterns were obtained using a JEOL 2000 FX electron microscope, provided with a double-tilt $\pm 45^\circ$ goniometer.

An *in situ* X-ray diffraction experiment was performed during the discharge of a cell with configuration Li/1 M $LiPF_6$ in EC + DMC (2:1)/$Li_2Ti_3O_7$ + C + PVDF-HFP (72%, 8%, 20% w/o, respectively) which has a beryllium window in contact with the cathode (9). The conformation of the plastic positive electrode was done using Bellcore's Plastic Technology. The cell was connected to a MacPile system and placed in a Siemens D-5000 apparatus using Cu$K\alpha$ radiation. The cell was discharged down to 1 V by the application of a constant current corresponding to the insertion of 1 lithium ion per $Li_2Ti_3O_7$ formula unit every 60 h. X-ray diffraction patterns were collected between $2\theta = 5^\circ$–48° degrees, with a counting time of 8 s and step size of 0.02°. Therefore, each pattern was recorded during the insertion of 0.074 lithium ions in the active material.

RESULTS AND DISCUSSION

Figure 2 shows both the typical voltage–composition and the incremental capacity, dx/dE, curves obtained by discharging of a lithium cell, bearing $Li_2Ti_3O_7$ as the active material of the positive electrode, at -5 mV/h. Four regions, labeled as I, II, III, and IV, can be distinguished in the voltage–composition plot. Each of them is due to different reductive processes during the insertion reaction. The voltage drop observed in regions I and IV seems to indicate that a solid solution is formed in each of the corresponding composition ranges. On the other hand, the nature of the processes II and III is not clear from only the composition–voltage data. However, the nature of the reductive processes can be investigated from the respective chronoamperograms. Figure 3a shows both current intensity (left axis)

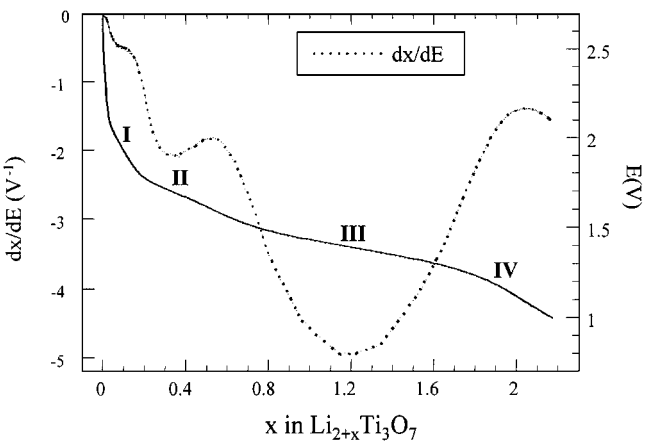

FIG. 2. Voltage composition curve (line) and incremental capacity (dots) of a cell Li/1 M $LiClO_4$ + DEE + EC (50:50)/$Li_2Ti_3O_7$ + C + EDPTP (89:10:1) discharged at -5 mV/h.

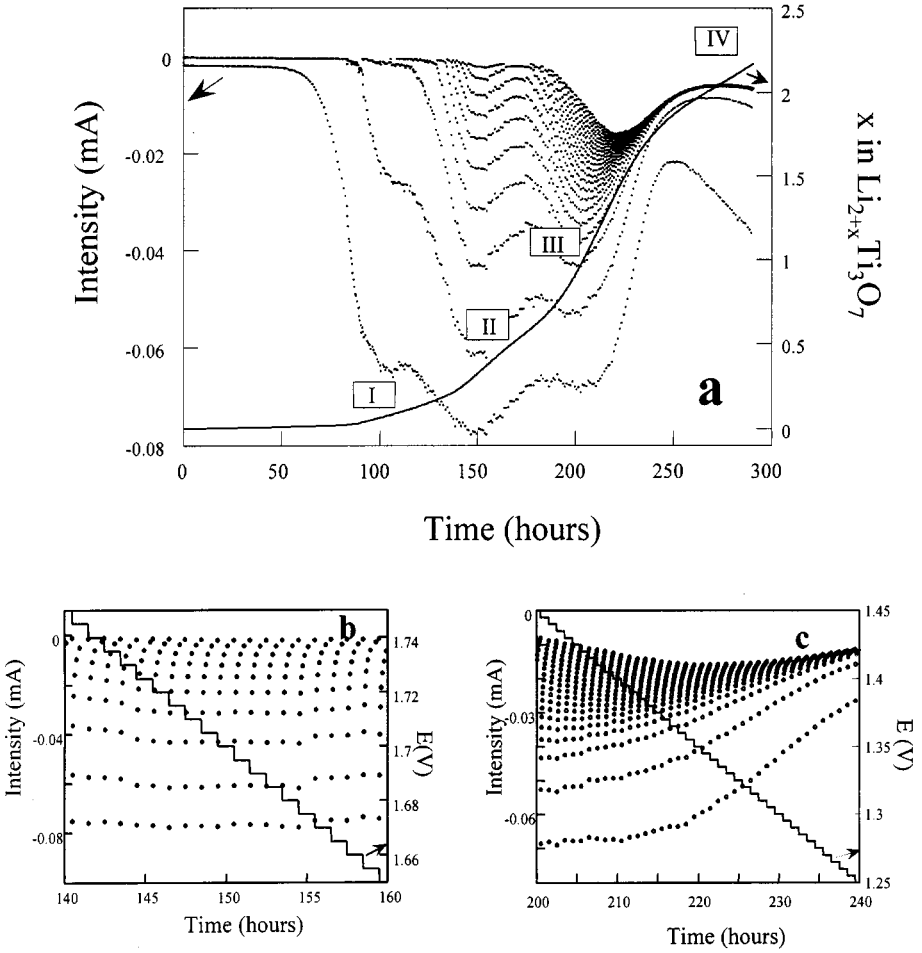

FIG. 3. (a) Time dependence of current (dots) and composition (line) during the discharge of a cell Li/1 M $LiClO_4$ + DEE + EC (50 : 50)/$Li_2Ti_3O_7$ + C + EDPTP (89 : 10 : 1) potentiostatically driven at − 5 mV/h steps. Details of the chronoamperogram showing the specific behavior of the reduction current crossing: (b) a two-phase domain and (c) a solid solution process.

and composition (right axis) time-dependence curves corresponding to the experiment of Fig. 2. During process II (see Fig. 3b) the time dependence of the current is the same at every voltage level, and the final current at every voltage step reaches the equilibrium condition (zero current). Both features indicate that the system is crossing a solid solution domain (10). On the other hand, the chronoamperogram obtained during process III (Fig. 3c) shows a different behavior. It must be attributed to the crossing of a two-phase region: the different shape of the relaxation curves on both sides of the minima (located at approximately 1.37 V), and the presence of a non-faradic residual current at each potential level (11). We have not obtained information about process I and IV using this data since current density decreases very rapidly during the corresponding voltage steps, and only a small number of points were collected. However, the abrupt voltage drops observed in these two regions indicate that solid solutions may be formed in both cases. Therefore, keeping in mind the composition range of the voltage–composition plot shown in Fig. 2 we can deduce, for each of the detected processes, the approximate extension of the corresponding regions:

Region I	$Li_{2+x}Ti_3O_7$	$0 < x < 0.2$	Solid solution
Region II	$Li_{2+x}Ti_3O_7$	$0.2 < x < 0.6$	Solid solution
Region III	$Li_{2+x}Ti_3O_7$	$0.6 < x < 1.9$	Biphasic region
Region IV	$Li_{2+x}Ti_3O_7$	$1.9 < x < 2.25$	Solid solution

The existence of two consecutive monophasic regions at the beginning of the insertion process may be understood if one thinks of the formation of an ordered arrangement of lithium ions at the limiting composition between these two solid solutions (12). In our case it would be close to $x = 0.2$. For better detection of the compositions that produce ordered structures, the variation of incremental capacity with composition, dx/dE vs x, is shown in Fig. 2. We have to take into account that the incremental capacity presents a maximum during the formation of a solid solution when an ordering of lithium is set (13).

Analysis of the incremental capacity variation shown in Fig. 2 gives the following result. A first maximum, which may correspond to the border between region I and II, is not well defined because only a shoulder, indicating its presence, is observed around 0.15. A second maximum appears close to the high limit of region II, since it is located at 0.55. Finally around $x = 2$, close to the border between regions III and IV a new maximum, perhaps due to another ordering state, is observed. Hence we may assume that for the compounds with formulae $Li_{2+x}Ti_3O_7$ with $x = 0.55$ and 2.0, ordered arrays of lithium ions are present. Besides, another ordering state may exist for some value close to $x = 0.15$. We have looked for evidence of these ordering states by means of electron diffraction, as we will also show.

Once the composition $Li_{2+0.55}Ti_3O_7$ has been obtained, the insertion reaction goes on through a two-phase region, the final composition limit of which has not been well established in this work since we have observed that it depends on the experimental conditions of the electrochemical run (14). For the slowest experiments performed, this limit is reached at $x = 2$. After a possible ordering state, $Li_{2+x}Ti_3O_7$ with $x \approx 2$, the final solid solution (region IV) begins to form. According to the formula $(Li_{1.72}\square_{2.28})$ tunnel $[(Li_{0.57}Ti_{3.43})O_8]$ framework, the total occupancy of the ramsdellite tunnel should be achieved when two lithium ions are inserted in $Li_2Ti_3O_7$ (6). Therefore, because more than that quantity can be inserted in $Li_2Ti_3O_7$, one wonders whether the ramsdellite framework is still maintained.

The structural characterization of the $Li_{2+x}Ti_3O_7$ phases was initially performed by means of powder X-ray diffraction. Figure 4 shows a set of *in situ* X-ray diffraction patterns taken during the discharge of a lithium cell bearing $Li_2Ti_3O_7$ as the active material. The diffraction data show that the reflections of the starting compound, $Li_2Ti_3O_7$ (same as the ones appearing for $x = 0.04$), are present during the entire insertion reaction, although some changes are observed. For compositions lower than $x = 0.93$, a shift of some reflections (for instance 130 and 131) is consistent with the presence of a solid solution domain that was in fact detected by the electrochemical measurements. At approximately $x = 0.78$ some new peaks appear (marked with arrows) that cannot be indexed with the ramsdellite cell. Although for high lithium content ($x > 2$) the electrochemical data suggested the presence of only one phase, we first explored the possibility of phase segregation. However, the extra reflections could not be indexed with any of the probable segregation compounds (rutile, spinel, goethite, etc.). We may then assume, to be in agreement with the electrochemical measurement, that a single phase with a new structure is stabilized once the ramsdellite composition limit has been exceeded, i.e., for $x > 2$. However, since the $Li_2Ti_3O_7$ reflections are also present in the X-ray diffraction patterns, the new structure might keep a close relationship with the ramsdellite structure.

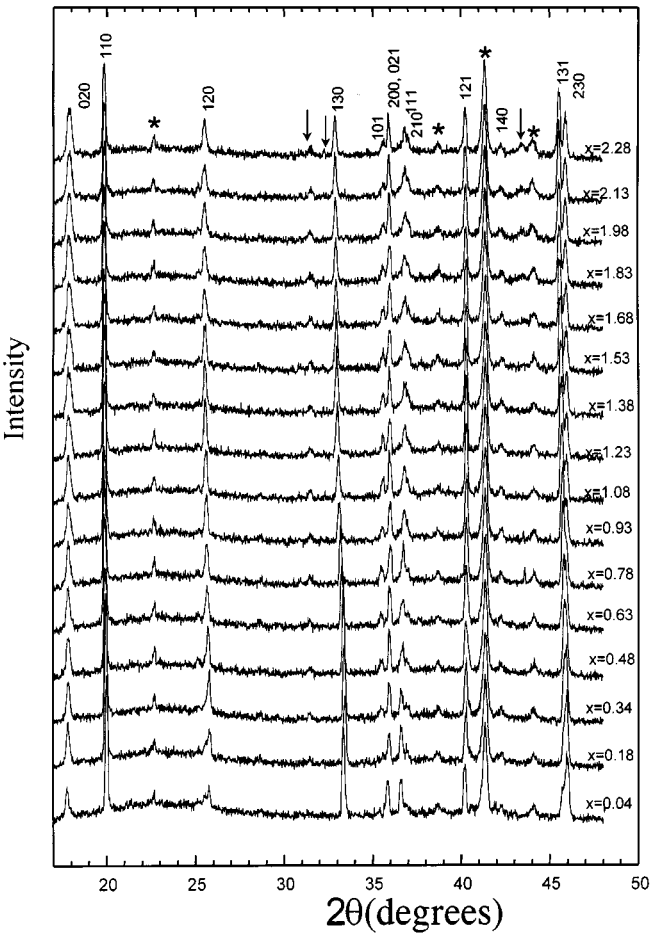

FIG. 4. X-ray diffraction data recorded for a Li/1 M $LiPF_6$ + EC + DMC (2:1)/$Li_2Ti_3O_7$ + C + PVDF-HFP (72:8:20) *in situ* cell. Peaks from $Li_2Ti_3O_7$ are indicated by their Miller indices, new peaks from $Li_{2+x}Ti_3O_7$ are signaled by arrows, and peaks from the *in situ* cell device are labeled with asterisks.

Lattice parameters were refined using the FULLPROF program but considering only the reflections of the ramsdellite-type structure. The space group and initial cell parameters were taken from the parent compound $Li_2Ti_3O_7$: $a = 5.0158(6)$ Å, $b = 9.548(1)$ Å, $c = 2.9460(4)$ Å, $V = 141.08(4)$ Å^3, space group *Pbnm*. The variation of the lattice parameters as a function of x is shown in Fig. 5. The a parameter decreases 1.6%, the b parameter increases 2.1%, and the c parameter decreases 1.5%, so that an overall compression of the unit cell of 2% is finally observed. One can compare this value with both, those obtained for the insertion of 0.9 lithium ion in the ramsdellite MnO_2, which produce a 21.4% change of cell volume (15), and those obtained for the insertion of 0.17 lithium ions in carbon, which produce a 9.4% change in volume (16), finally concluding that changes in cell parameters of $Li_2Ti_3O_7$ are not severe. Such slight changes in the unit cell indicate that

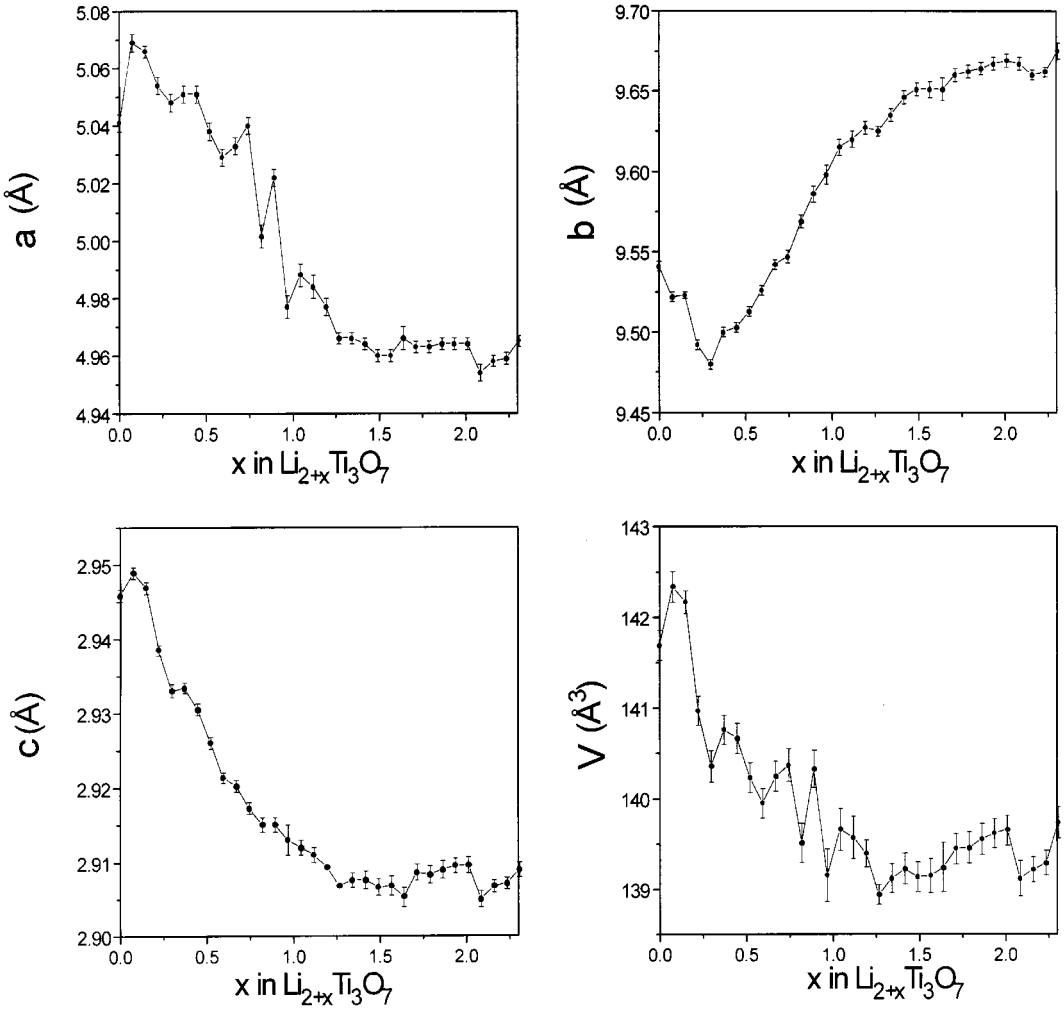

FIG. 5. Lattice parameters and volume of $Li_{2+x}Ti_3O_7$ as a function of lithium content, x.

the host compound is not going to suffer a hard structural stress over prolonged electrochemical cycling.

The variation of the cell parameters with composition (x) shows different trends as can be seen in Fig. 5. For $x < 1$ some of the parameters have an approximately linear dependence with the amount of inserted lithium, indicating a solid solution domain. Within this monophasic region, the slope of the variation of b parameter has opposite signs at both sides of the composition $x = 0.2$. This fact is consistent with two consecutive $Li_{2+x}Ti_3O_7$ solid solutions separated by the composition $Li_{2+0.2}Ti_3O_7$ as deduced from the voltage–composition curve. This composition is close to the possible ordered state detected by the analysis of the derivative curve around $x = 0.15$ (see Fig. 2). The electrochemical data also "predict" another "special" composition, $Li_{2+0.55}Ti_3O_7$, although no relevant feature has been detected in the X-ray diffraction data around this composition. Above $x = 1$ the variation of cell parameters is less abrupt and a tendency to a constant value can be observed; this is consistent with the presence of a two-phase region detected by electrochemical measurements at $0.6 < x < 1.9$. This trend seems to show an inflection point at $x = 2$, pointing out again the significance of this composition, at which the expected limit composition of the ramsdellite structure is reached. In any case, the lattice parameters for compounds with high lithium contents are just orientative since, although another reflections are present, we have only considered the basic ramsdellite reflections. This has been done in order to analyze the changes in the same unit cell during the entire insertion process. This calculation would be only valid under the assumption that the final compound has a closely related ramsdellite-type structure. As we show below this is effectively the case.

The microstructure of several compounds $Li_{2+x}Ti_3O_7$, belonging to the different regions mentioned above, was studied by selected area electron diffraction. As the first

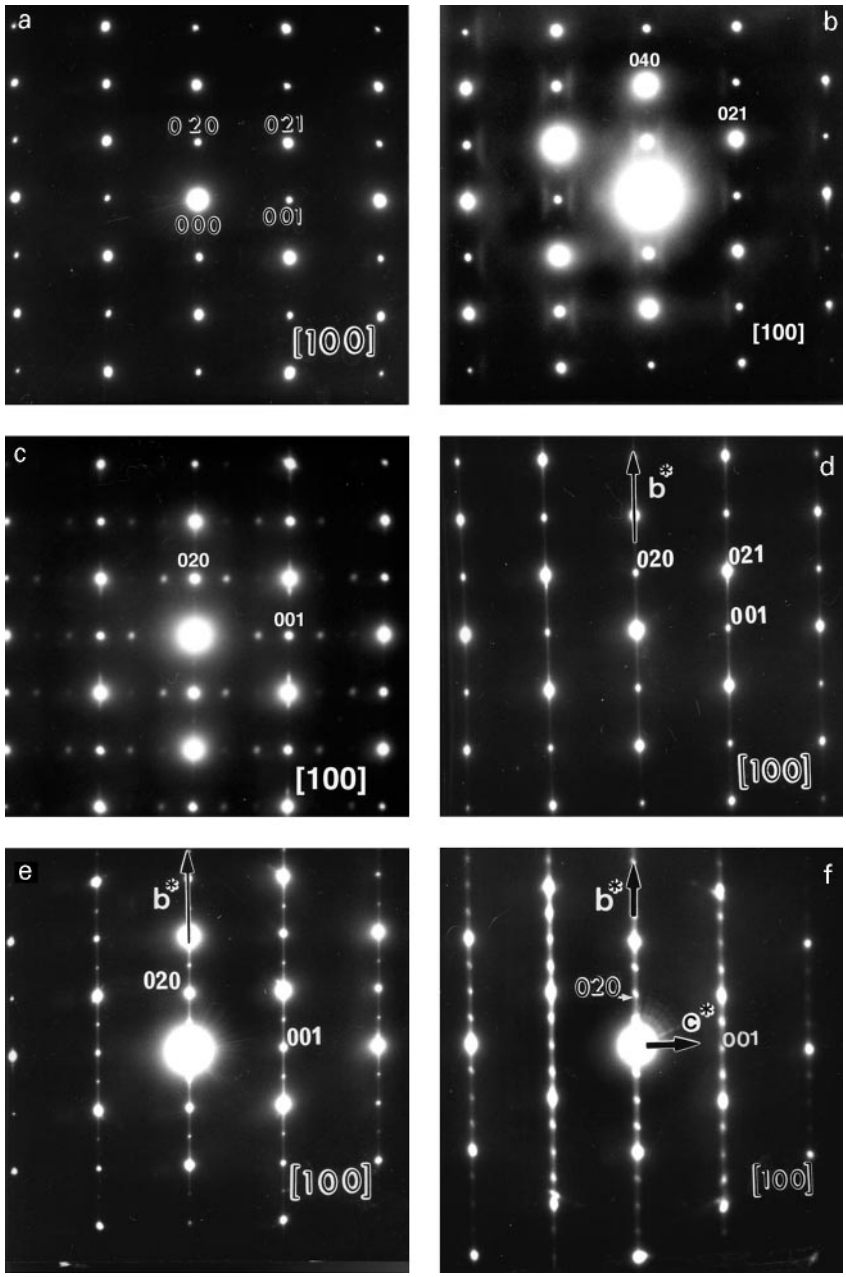

FIG. 6. Electron diffraction patterns along the [100] zone axis for $Li_{2+x}Ti_3O_7$ with (a) $x = 0, 0.1$, (b) $x = 0.25, 0.35$, (c) $x = 0.55$, (d) $x = 0.8$, (e) $x = 1.6$, and (f) $x = 2.2$. For all of these samples, x refers to average composition (see text).

result we can say that, in spite of the experimental conditions used to approch equilibrium, the synthesized samples are inhomogeneous, since for each prepared composition different, although related, types of crystallites were found. It is for this reason that we have to consider hereafter the prepared compositions as average compositions. With this limitation in mind, we report the results for electrochemically obtained $Li_{2+x}Ti_3O_7$ ($0.1 \leq x \leq 2.2$) samples. This study allowed us to track the different types of crystals that are being formed while the system is crossing the different regions. We have selected the most representative pattern for every studied sample by choosing that which is found for most of the crystals. In this way, Fig. 6 shows a set of patterns taken along the ramsdellite [100] zone axis of the different types of crystals. Figure 6a corresponds to an electron diffraction pattern characteristic of the starting compound $Li_2Ti_3O_7$, and it is also the only type obtained for the "$Li_{2+0.1}Ti_3O_7$" composition. Therefore, as expected, the microstructure of the host compound is not affected by such a low amount of inserted lithium.

For the average compositions $Li_{2+x}Ti_3O_7$, with $x = 0.25$ and 0.35, most of the crystals exhibit, along the [100] zone axis, a pattern such as the one shown in Fig. 6b. In this pattern, the spots of the starting compound $Li_2Ti_3O_7$ can be seen again, although a new feature is observed: the existence of some diffuse scattering around every reflection. This effect was still observed when the crystals were tilted while maintaining either the b^* or the c^* direction. Therefore, it must be interpreted as a tridimensional effect in reciprocal space. Normally, the diffuse scattering is due to short-range ordering that may evolve to long-range ordering as observed in other reported cases (17,18). The detected diffuse intensity could be due to short-range order between the two ordered states that may exist for $Li_{2+x}Ti_3O_7$ with $x \approx 0.15$ and $x = 0.55$. Although another samples with x between 0.1 and 0.2 were examined for any long-range ordering that could be assigned to $Li_2Ti_3O_7$ with $x \approx 0.15$, we did not find any evidence of it. On the contrary, the existence of an ordering state was found for much higher lithium content ($x = 0.55$).

For the sample "$Li_{2+0.55}Ti_3O_7$" we found patterns such as the one shown in Fig. 6c. In addition to the intense spots of the ramsdellite basic cell, some weak spots appear along the c^* direction that could not be interpreted with that cell. The intensity distribution of these extra spots indicates the existence of an incommensurable modulation ($q \approx \frac{1}{3}c^*$). As happens in other inserted compounds (19), this modulation could originate by an ordering of lithium ions at a composition that is consistent with our electrochemical data.

For the composition $x = 1.6$ the lack of homogeneity is larger than for the samples with lower lithium contents: some crystals present the Fig. 6b pattern, others present the Fig. 6d pattern, and even a third kind of pattern, Fig. 6e, is found. This mixture of crystals supports the existence of a multiphasic region that was detected by the electrochemical measurements with approximate compositional limits $Li_{2+0.6}Ti_3O_7$ and $Li_{2+1.9}Ti_3O_7$. Obviously samples belonging to this region have to contain a mixture of these latter two compounds. Therefore, the electron diffraction patterns of Fig. 6d and 6e should correspond to the upper limit, $Li_{2+1.9}Ti_3O_7$, which is also the initial composition of the solid solution $Li_{2+x}Ti_3O_7$, with $1.9 < x < 2.25$. In agreement with this assumption, in the sample of nominal composition $Li_{2+2.2}Ti_3O_7$ (a sample that belongs to the solid solution with high lithium content) crystals displaying Fig. 6d and 6e patterns have been found. The pattern in Fig. 6d maintains the spots of the host compound (see Fig. 6a) although the appearance of streaking along the (010) direction reveals a disordering of planes perpendicular to this direction. This streaking is also present in the pattern of Fig. 6e, although some differences are observed. New reflections are present along the b^* direction for which two possible interpretations can be made. The first is that these new spots are, in fact, the $0k0$ reflections with $k = 2n + 1$, which are forbidden by the space group of the ramsdellite structure (*Pbnm*). This would imply a change of the cell symmetry. In the second interpretation the extra spots are interpreted as an effect of a doubling of the b ramsdellite lattice parameter, i.e., the indexing can be made by using the orthorhombic cell $a \times 2b \times c$. This new cell may have its origin in a lithium ordering that we relate with the composition $Li_{2+2}Ti_3O_7$, since for $x = 2$ a maximum in the dx/dE versus x plot was observed (see Fig. 2). Although the location of lithium and hence the determination of the structure is a problem that could be solved by neutron diffraction, the heterogeneity of the samples did not allow such studies to be undertaken.

Figure 6f shows the most characteristic electron diffraction pattern of the highly lithiated compound $Li_{2+2.2}Ti_3O_7$ in the same orientation, i.e., the [100] zone axis. As expected, the same features as in Fig. 6e can be observed, although here the extra spots are more intense. As explained for the previous composition, the interpretation of this pattern makes necessary a new cell that in any of the proposed possibilities is closely related with the cell of the parent compound $Li_2Ti_3O_7$. This new cell is formed when lithium content reaches very high values, i.e., at the minimum voltage that is reached when a lithium battery, having $Li_2Ti_3O_7$ as active material, is cycled. This may account for the good reversibility of the intercalation reaction of lithium in $Li_2Ti_3O_7$.

CONCLUSIONS

During the insertion of 2.24 lithium ions in the ramsdellite $Li_2Ti_3O_7$, several processes have been electrochemically detected. The upper composition limit for the ramsdellite structure, $Li_{2+2}Ti_3O_7$, is obtained through two consecutive solid solutions and a biphasic region. Structural characterization has shown that all the intermediate lithiated phases maintain the basic ramsdellite structure, although some evidence of lithium ordering has been found. For example, an incommensurate modulation ($q \approx \frac{1}{3}c^*$) has been found for a sample with average composition $Li_{2+0.55}Ti_3O_7$.

Once the composition $Li_{2+2}Ti_3O_7$ is exceeded, X-ray diffraction data show that a new structure is stabilized. The electron diffraction study unambiguously shows that the new structure is closely related to the ramsdellite structure. The slight change in the volume of the basic cell, 2%, accounts for the good cyclability of $Li_2Ti_3O_7$ as an electrode material.

ACKNOWLEDGMENTS

We thank CICYT (MAT 95/0809 and MAT98-1053-C04) and Universidad San Pablo-CEU for financial support. We also thank Prof. J. M. Tarascon and Dr. S. Denis for making possible the *in situ* X-ray diffraction experiments at the Universite de Picardie Jules Verne.

REFERENCES

1. B. Morosin and J. C. Mikkelsen, *Acta Crystallogr. B* **35,** 798 (1979).
2. I. Abrahams, P. G. Bruce, W. I. F. David, and A. R. West, *J. Solid. State Chem.* **78,** 170 (1989).
3. C. J. Chen and M. Greenblatt, *Mater. Res. Bull.* **20,** 1347. (1985).
4. S. Garnier, C. Bohnke, O. Bohnke, and J. L. Fourquet, *Solid State Ionics* **83,** 323 (1996).
5. M. E. Arroyo y de Dompablo, E. Morán, A. Várez, and F. García-Alvarado, *Mater. Res. Bull.* **32,** 993 (1997).
6. J. Grins and A. R. West, *J. Solid State Chem.* **65,** 265 (1986).
7. H. Kawai, M. Nagata, H. Tukamoto, and A. R. West, *J. Mater. Chem.* **8(4),** 837 (1998).
8. C. Mouget and Y. Chabre, Multichannel Potentiostatic and Galvanostatic System MacPile, licensed by CNRS and UJF Grenoble to Bio-Logic Corp. , 1 Avenue de l'Europe, F-38640 Claix, France, 1991.
9. S. Denis, E. Baudrin, M. Touboul, and J. M. Tarascon, *J. Electrochem. Soc.* **144,** 4099 (1997).
10. Y. Chabre, "Chemical Physics of Intercalation II," *in* NATO ASI Series 305, p. 181. Springer-Verlag, Berlin, 1992.
11. G. B. M. Vaughan, M. Barral, T. Pagnier, and Y. Chabre, *Synth. Met.* **77,** 7 (1996).
12. A. H. Thompson, *J. Electrochem. Soc.* **216,** 608 (1979).
13. A. J. Berlinsky, W. G. Unruh, W. R. McKinnon, and R. R. Haering, *Solid State Commun.* **31,** 135 (1979).
14. M. E. Arroyo y de Dompablo, Doctoral Thesis, Universidad Complutense de Madrid, 1998.
15. M. M. Thackeray, *Prog. Solid State Chem.* **25,** 1 (1997).
16. D. Fatuteux and R. Koksbang, *J. Appl. Electrochem.* **23,** 1 (1993).
17. R. De Ridder, G. Van Tendeloo, and S. Amelinckx, *Acta Crystallogr. A* **32,** 216 (1976).
18. A. K. Larsson, R. L. Withers, and L. Stenberg, *J. Solid State Chem.* **127,** 222 (1996).
19. J. P. Peres, F. Weill, and C. Delmas, *Solid State Ionics* **116,** 19 (1999).